INTERFACE FOCUS

rsfs.royalsocietypublishing.org

Research

Cite this article: Verre AF, Faroni A, Iliut M, Silva C, Muryn C, Reid AJ, Vijayaraghavan A. 2018 Improving the glial differentiation of human Schwann-like adipose-derived stem cells with graphene oxide substrates. *Interface Focus* **8**: 20180002.
http://dx.doi.org/10.1098/rsfs.2018.0002

Accepted: 31 January 2018

One contribution of 13 to a theme issue 'The biomedical applications of graphene'.

Subject Areas:
nanotechnology

Keywords:
adipose stem cells, graphene, glial differentiation

Author for correspondence:
Aravind Vijayaraghavan
e-mail: aravind@manchester.ac.uk

THE ROYAL SOCIETY PUBLISHING

Improving the glial differentiation of human Schwann-like adipose-derived stem cells with graphene oxide substrates

Andrea Francesco Verre[1], Alessandro Faroni[3], Maria Iliut[1], Claudio Silva[1,4], Cristopher Muryn[2], Adam J. Reid[3,5] and Aravind Vijayaraghavan[1]

[1]School of Materials and National Graphene Institute, and [2]School of Chemistry, University of Manchester, Manchester M13 9PL, UK
[3]Blond McIndoe Laboratories, Division of Cell Matrix Biology and Regenerative Medicine, School of Biological Sciences, Faculty of Biology Medicine and Health, University of Manchester, Manchester Academic Health Science Centre, Manchester M13 9PL, UK
[4]Department of Fundamental Chemistry, Institute of Chemistry, University of São Paulo, São Paulo, Brazil
[5]Department of Plastic Surgery and Burns, Wythenshawe Hospital, Manchester University NHS Foundation Trust, Manchester Academic Health Science Centre, Manchester, UK

AF, 0000-0003-4435-6423; MI, 0000-0003-0786-6408; CS, 0000-0003-4331-3755; AJR, 0000-0003-1752-3302; AV, 0000-0001-8289-2337

There is urgent need to improve the clinical outcome of peripheral nerve injury. Many efforts are directed towards the fabrication of bioengineered conduits, which could deliver stem cells to the site of injury to promote and guide peripheral nerve regeneration. The aim of this study is to assess whether graphene and related nanomaterials can be useful in the fabrication of such conduits. A comparison is made between graphene oxide (GO) and reduced GO substrates. Our results show that the graphene substrates are highly biocompatible, and the reduced GO substrates are more effective in increasing the gene expression of the biomolecules involved in the regeneration process compared to the other substrates studied.

1. Introduction

Schwann cells (SC) are key cellular elements in assisting the regeneration of peripheral nerve after injury. SC switch from a myelinating to repair phenotype which results in increased expression of extracellular matrix (ECM) proteins, neurotrophins and growth factors; furthermore, SC undergo profound morphological changes which result in upregulation of filament cytoskeletal proteins such as nestin and actin [1,2]. Despite a clear need for novel therapies, use of SC as a clinical intervention for peripheral nerve injury is problematic due to the necessity of harvesting a functional nerve and the limited expansion capacity of SC. As a clinically viable alternative, mesenchymal stem cells and adipose-derived mesenchymal stem cells (ASCs) have been differentiated *in vitro* towards a Schwann-like cells phenotype [3,4]. These differentiated adipose stem cells (dASCs) express glial markers such as glial fibrillary acidic protein, S100 and p75 [4]; express myelin protein [5] and myelin structures when in co-culture with neurons [6,7]; and when implanted in bioengineered conduits to repair murine peripheral nerve gap *in vivo*, dASCs have demonstrated promotion of nerve regeneration, reduction of muscle atrophy, increased nerve conduction velocity and higher rates of myelination [8–11].

Graphene and related nanomaterials can play an important role in the fabrication of bioengineered nerve conduits for the treatment of peripheral nerve injuries. Although the biocompatibility of these materials for *in vivo* studies depends on many variables such as the thickness, the lateral size of the flakes, the level of hydrophilicity and the extent of functionalization [12], it can be stated that when these materials were used as coatings on surfaces to support stem cell growth, the extent of cytotoxicity was limited and enhanced stem cell differentiation was

reported [13–17]. Graphene and related nanomaterials were found to be effective in positively modulating axonal outgrowth and nerve regeneration *in vitro* [18–21]. Thus far, researchers have been exploring the effect of graphene and related nanomaterials on the neurite outgrowth, but there have not been studies regarding the effect of these materials in supporting the growth of dASCs. The aim of this study is then the biological characterization of graphene oxide (GO) and reduced GO (rGO) coated coverslips and to verify if these materials are able to sustain the dASC phenotype, which is rapidly lost following withdrawal of growth factors [22].

2. Material and methods

2.1. Graphene-based materials synthesis, substrates preparation and characterization

Graphite oxide was synthesized by a modified Hummers method [23,24] and exfoliated down to constituent monolayers to yield GO. Glass coverslips were washed in a sonication bath with Decon® 90 for 15 min followed by deionized (DI) water for another 15 min and finally with isopropanol for 15 min. After the coverslips were dried, they were treated for 5 min in oxygen plasma to increase the hydrophilicity of the coverslips. GO dispersions were then spin-coated on the glass coverslips at a concentration of 2 mg ml^{-1} at 2500 r.p.m., 250 r.p.m. s^{-1} acceleration for 2 min. To obtain rGO coverslips, GO coverslips were kept for 3 days at 180°C in vacuum. Atomic force microscopy (AFM) measurements were carried using a Bruker FastScan microscope in tapping mode. Raman spectroscopy was performed using a Renishaw inVia Raman microscope with 532 nm laser excitation. X-ray photoelectron spectroscopy (XPS) spectra of drop-cast substrates were recorded with a SPECS NAP-XPS system employing a monochromatic Al Kα source (1486.6 eV). Before the biological experiments, the coverslips were sterilized by immersion in pure ethanol then washed in DI water and then left to dry under a hood.

2.2. Human adipose stem cell harvesting and differentiation

ASCs were isolated according to a previously reported protocol [4]. Human abdominal, subcutaneous adipose tissue was harvested from three female surgical patients undergoing reconstructive surgery at the University Hospital of South Manchester, UK. All patients were fully consented and procedures approved by the National Research Ethics Committee, UK (NRES 13/SC/0499). Adipose tissue biopsies were minced by a razor blade and dissociated by an enzymatic treatment of 0.2% (w/v) of collagenase I (Life Technologies, Paisley, UK) for 60 min at 37°C under constant agitation. The digested tissue was then filtered through a vacuum-assisted 100 µm nylon mesh (Merck Millipore, Watford, UK). An equal volume of stem cell growth medium containing a-minimum essential Eagle's medium (aMEM) (Sigma-Aldrich, Poole, UK), 10% (v/v) fetal bovine serum (LabTech, Uckfield, UK), 2 mM L-glutamine (GE Healthcare UK, Little Chalfont, UK) and 1% (v/v) penicillin–streptomycin was added. The solution was centrifuged at 300*g* for 10 min and the resulting pellet was suspended in 1 ml of Red Blood Cell Lysis Buffer (Sigma-Aldrich) for 1 min, and 20 ml of aMEM was added to arrest lysis. The mixture was centrifuged at 300*g* for 10 min, and the resulting pellet was resuspended in aMEM and plated in T75 flasks for cell culture. Cells were routinely characterized for the expression of stem cell surface markers as per [22].

The differentiation of ASCs towards dASCs was performed following a previously reported protocol [4]. Briefly, ASCs at the passage 1–2 at 30% of confluence were treated with 1 mM β-mercaptoethanol (Sigma-Aldrich) for 24 h, then with 35 ng ml^{-1} of all-*trans*-retinoic acid for 72 h. After this initial treatment, ASCs were treated by 5 ng ml^{-1} of platelet-derived growth factor (Peprotech EC, London, UK), 10 ng ml^{-1} basic fibroblast growth factor (Peprotech EC), 14 µM of forskolin (Sigma-Aldrich) and 192 ng ml^{-1} glial growth factor (GGF-2) (Acorda Therapeutics, Ardsley, NY, USA). ASCs were kept under these conditions for two weeks, replacing media every 72 h and passaging when confluence was reached.

2.3. Cell proliferation and live/dead assays

To assess cell proliferation rate by the 3-(4,5-dimethylthiazol-2-yl)-5-(3-carboxymethoxyphenyl)-2-(4-sulfophenyl)-2H-tetrazolium (MTS) assay, dASCs were plated at a concentration of 5000 cells per coverslip in triplicate on the sterilized graphene-coated coverslips. The coverslips were put in ultra-low adherence 24-well cell plates to avoid attachment of the cells to the tissue culture plastic underneath the coverslips. At days 1, 4 and 7 after seeding, the cell medium was aspirated and cells were washed in phosphate-buffered saline (PBS). After the washing step, the cells were incubated in 20% (v/v) CellTiter 96 Aqueous One Solution Cell Proliferation Assay (Promega, Southampton, UK), diluted in phenol-free DMEM (Sigma-Aldrich) for 90 min in the dark at 37°C. After the incubation, the absorbance at 490 nm was recorded using an Asys UVM-340 microplate reader/spectrophotometer (Biochrom, Cambridge, UK). For the viability assays, ASCs were plated at a concentration of 25 000 cells per coverslip in triplicate in a cell medium containing α-MEM and 1% (v/v) P/S without growth factors. After 48 h, the medium was aspirated and the cells were washed in PBS. Calcein-AM fluorescein and ethidium homodimer-1 (Eth-D1) purchased from LIVE/DEAD® Viability/Citoxicity Kit (Molecular Probes, Invitrogen, UK) were added at a concentration of 0.5 and 2 µg ml^{-1}, respectively, in PBS and left to react for 15 min at 37° C. After this step, images were taken using a fluorescence inverted microscope (Olympus IX51, Japan) under 4× magnification. Data from MTS experiment were expressed as absorbance at 490 nm ± s.e. of the mean ($n = 3$), while data from viability assay were expressed as percentage of live cells measured by dividing the average green stained area by the average of the whole (live + dead) stained area, measured with ImageJ software (v. 1.48) multiplied by 100.

2.4. Quantitative real-time polymerase chain reaction

For gene expression studies, cells were seeded as above at a concentration of 50 000 cells per coverslip in triplicate and the RNA was extracted after 48 h of cellular growth on the different coverslips. RNA was extracted using the RNeasy Plus Mini Kit (Qiagen) following the instruction of the manufacturer. The concentration of the RNA was quantified using a NanoDrop ND-100 (Thermo Fisher Scientific, Waltham, MA, USA) spectrophotometer. One microgram of each sample was reverse transcribed using an RT2 First Strand Kit (Qiagen) following the instruction of the manufacturer. DNA elimination steps were included in both RNA extraction and cDNA synthesis to prevent downstream genomic DNA amplification. Quantitative real-time polymerase chain reaction was performed with RT2 SYBR Green qPCR Mastermix (Qiagen) and a Corbett Rotor Gene 6000 (Qiagen), by the use of the following protocol: hot start for 10 min at 95°C, followed by 40 cycles of 15 s at 95°C, annealing for 30 s at 55°C and extension for 30 s at 72°C. To verify the specificity of the reactions, a melting curve was obtained with the following protocol: 95°C for 1 min, 65°C for 2 min, and a gradual temperature increase from 65°C to 95°C (2°C min^{-1}). Data were normalized for the housekeeping gene, and the $\Delta\Delta$Ct method was used to determine the fold changes in gene expression with glass coverslips as controls. The primer assays were obtained from Qiagen as reported in the literature [22].

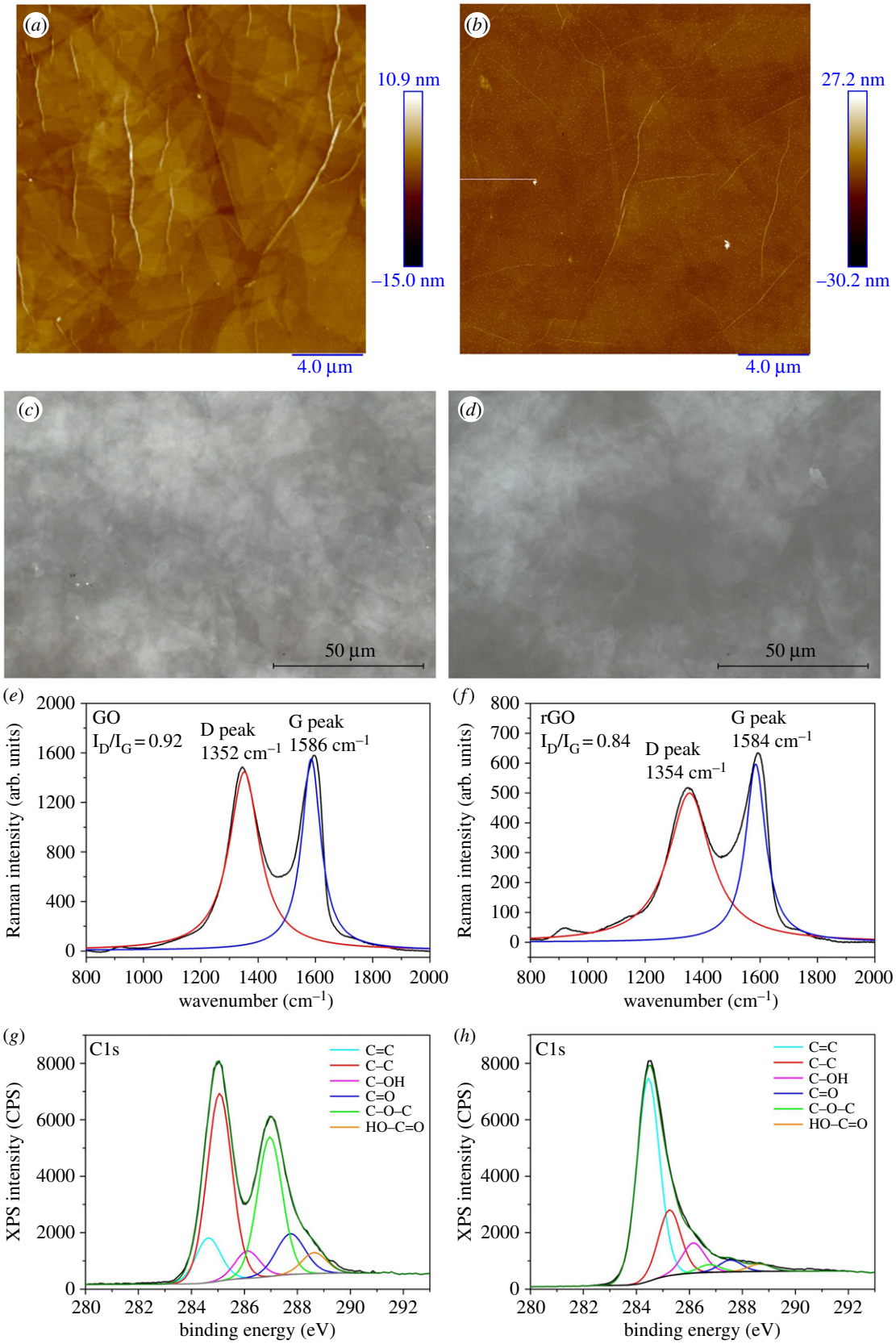

Figure 1. (*a*,*b*) AFM topography images of GO and rGO substrates, respectively; (*c*,*d*) optical images of GO and rGO substrates, respectively; (*e*,*f*) Raman spectra of GO and rGO substrates, respectively; (*g*,*h*) XPS C1s spectra of GO and rGO-coated substrates, respectively.

2.5. Statistical analysis

Statistical significance of the studies was evaluated by the use of GraphPad Prism 6.0 (GraphPad Software, La Jolla, CA, USA) using a one-way ANOVA test followed by Dunnett's multiple comparison test using glass as a control sample. Level of significance was expressed as *p*-values.

3. Results and discussion

3.1. Substrates characterization

Optical microscopy and AFM showed the uniformity of thin film coverage on the substrate and no empty areas were observable on the substrates as shown in figure 1*a*–*d*. Raman

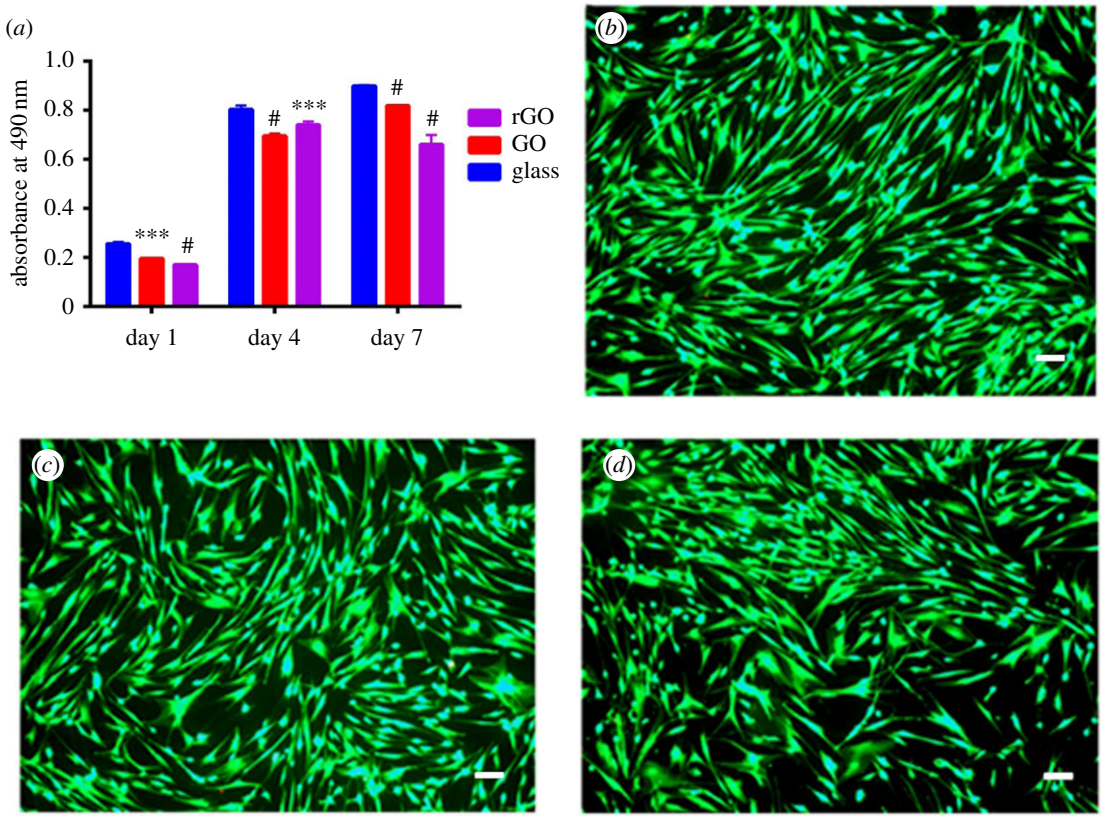

Figure 2. (*a*) MTS proliferation assay of dASCs grown on rGO (purple), GO (red) and glass (blue) substrates at day 1, at day 4 and day 7 time-points; $^{\#}p < 0.0001$, $^{***}p < 0.001$, $^{**}p < 0.01$, $^{*}p < 0.05$; (*b–d*) dASCs after 48 h of cellular growth on glass, GO and rGO, respectively. Calcein AM-positive cells are alive cells and they are visible in the image due to green fluorescence. 99.89 ± 0.01% of cells on GO substrates, 99.80 ± 0.02% of cells rGO coverslips and 99.87 ± 0.02% of cells on glass substrates were alive. Scale bar, 100 µm.

spectroscopy is a useful tool to detect the presence of GO on any surfaces. The typical spectrum of GO is composed by two peaks: the D peak at approximately 1350 cm^{-1} and the G peak at approximately 1586 cm^{1}. The intensity ratio (I_D/I_G) between these two peaks is employed to characterize GO dispersions. The measured I_D/I_G of GO was 0.92 while upon thermal reduction we noted a decreased I_D/I_G down to 0.84 (figure 1*e,f*). XPS C1s spectra of all the different substrates can be deconvoluted into six components: C=C (sp^2 carbon) at 284.6 eV, C–C (sp^3 carbon) at 285.1 eV, C–OH at 286 eV, C–O–C at 286.9 eV, C=O at 287.7 eV and HO–C=O at 288.8 eV (figure 1*g*) [25,26]. Successful reduction is confirmed by the C1s spectrum of rGO: we noted a clear decrease in all the oxygen functionalities with the exception of hydroxyl group, a decrease in sp3 carbon and increased sp2 carbon as shown in figure 1*h*. As previously reported [14], graphene-based materials are efficient materials for the fabrication of artificial scaffolds in regenerative medicine. In fact, graphene and related nanomaterials are characterized by ultra-high specific surface area and by the ability to bind stem cell growth inducers both covalently and non-covalently acting as a pre-concentration platform for growth factors and other biomolecules present in the differentiation medium. Starting from this observation, human dASCs were cultured on the substrates to assess cell proliferation and the effect of the substrate on the gene expression of glial markers.

3.2. Proliferation of dASCs on graphene substrates

To assess dASC proliferation rate on the different substrates studied, we used MTS assay. We selected three time-points on day 1, day 4 and day 7 after seeding. As can be seen in figure 2*a*, the proliferation rate of dASCs on both GO and rGO substrates was comparable to glass coverslips used as controls with values only marginally lower at each time point. To assess the biocompatibility of the substrates and confirm that the slightly reduced proliferation was not due to GO/rGO cytotoxicity, we performed a live/dead viability assay after 48 h of cellular growth on the different substrates. Indeed at each time point, we measured that 99.89 ± 0.01% of cells were alive on GO substrates, 99.80 ± 0.02% of cells were alive on rGO coverslips and finally 99.87 ± 0.02% of cells were alive on glass substrates. We can therefore conclude that although the proliferation rate was marginally slower on the rGO and GO coverslips, the amount of live cells was very high and comparable in all the different substrates studied. We then decided to study the gene expression of crucial proteins and growth factors which are key features of the differentiated state of dASCs and are involved in the peripheral nerve regeneration process.

3.3. Gene expression studies

Key molecules involved in the regeneration process are neurotrophins. These growth factors are involved in neuronal survival, development and functionality [27–29]. We decided to focus our attention studying brain-derived neurotrophic factor (BDNF), nerve growth factor (NGF) and glial-derived neurotrophic factor (GDNF). Also another group of protein molecules involved in the regeneration process are intermediate filament proteins such as nestin and vimentin, which are strictly related to the profound morphological changes associated with SC response to injury.

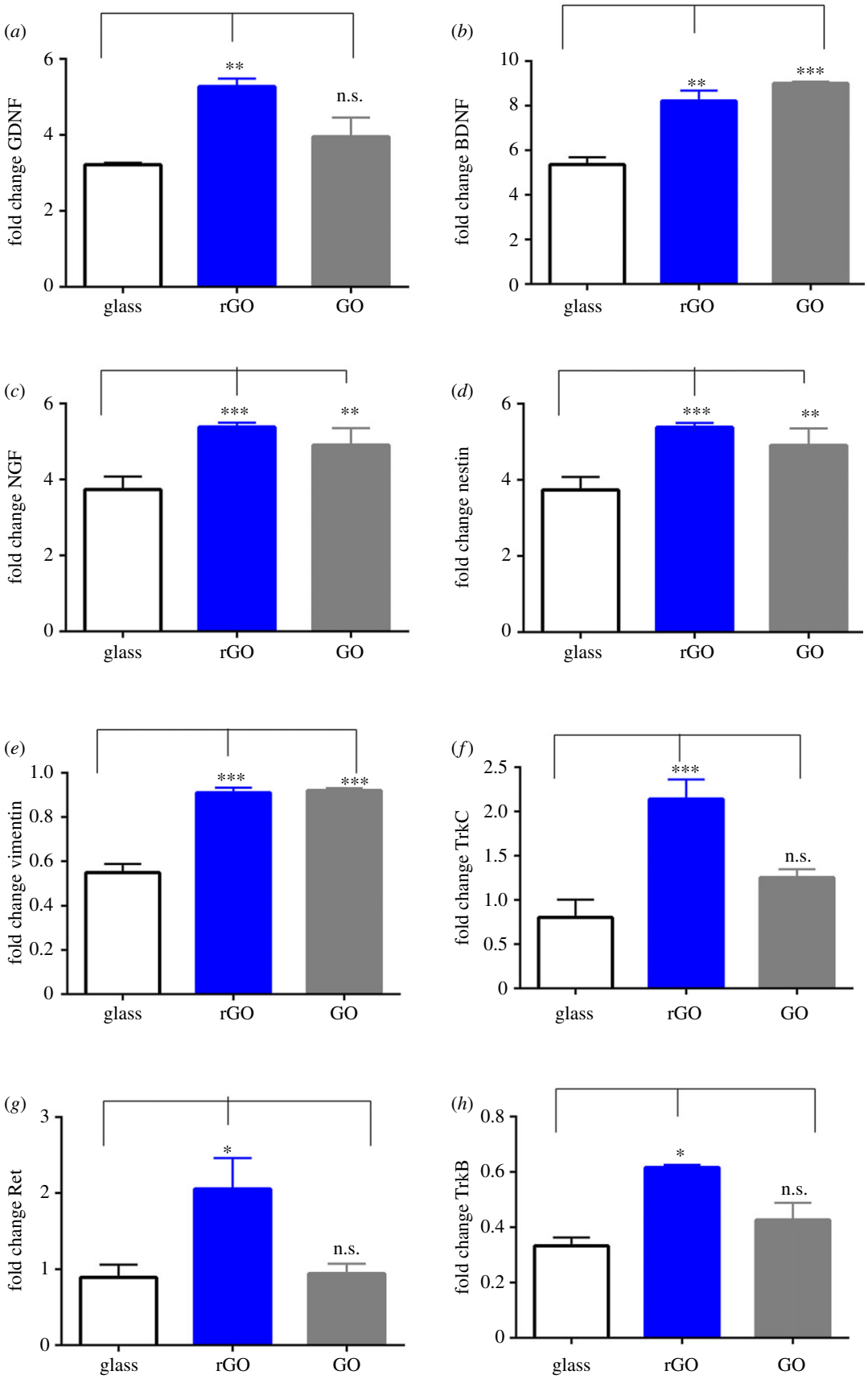

Figure 3. Gene expression after 48 h of dASC growth on glass, GO and rGO substrates for the following glial markers: (*a*) increased expression of GDNF on rGO substrates; (*b*) increased expression of BDNF on both GO and rGO substrates; (*c*) increased expression of NGF on rGO; (*d*) increased expression of nestin on both GO and rGO substrates; (*e*) increased expression of vimentin on both GO and rGO substrates; (*f*) increased expression of TrkC receptor on rGO substrates; (*g*) increased expression of Ret receptor on rGO substrates; (*h*) increased expression of TrkB receptor on rGO substrates. ***$p < 0.001$, **$p < 0.01$, *$p < 0.05$ and n.s., non-significant. Experiments were performed in triplicate.

Nestin is a protein which is involved in the axonal growth and is normally upregulated after nerve injury [30–33]. Moreover, a recent study highlighted that nestin-positive hair-follicle pluripotent stem cells were able to promote peripheral nerve regeneration [34]. Interestingly, a bigger proportion of ASCs were found to express nestin filaments compared to

bone marrow mesenchymal stem cells [4]. Vimentin is reported to be upregulated during peripheral nerve regeneration and higher expression levels of this protein have been reported to augment the peripheral nerve regeneration [35]. Lastly, we decided to investigate also the gene expression of neurotrophin receptors such as TrkB, TrkC and Ret as a measure of growth factor responsiveness of dASCs.

GDNF expression is increased on rGO coverslips (1.64 ± 0.06 versus glass, $p < 0.01$, $n = 3$) and no statistical difference is observed between GO coverslips and the glass controls. The expression of BDNF is increased on rGO and GO coverslips (1.53 ± 0.08, $p < 0.01$ versus glass, $n = 3$ on rGO substrates and 1.68 ± 0.01, $p < 0.001$ versus glass, $n = 3$ on GO substrates). NGF expression increased on rGO coverslips (1.67 ± 0.14, p-value < 0.01) while GO substrates behaved as glass controls (figure 3*a–c*).

Nestin expression is increased on both rGO and GO substrates (1.44 ± 0.05, $p < 0.01$ versus glass, $n = 3$ on rGO substrates and 1.31 ± 0.11, $p < 0.05$ versus glass, $n = 3$ on GO substrates). Vimentin expression is increased on both rGO and GO substrates (1.66 ± 0.04, $p < 0.001$ versus glass, $n = 3$ on rGO substrates and 1.67 ± 0.01, $p < 0.001$ versus glass, $n = 3$ on GO substrates) (figure 3*d*,*e*).

TrkC expression is increased on rGO substrates (2.86 ± 0.29, $p < 0.01$ versus glass, $n = 3$) while no statistical difference is observed between GO substrates and the glass controls. The same trend is followed by the gene expression of TrkB receptor. The expression of this gene is increased on rGO substrates (1.85 ± 0.02, $p < 0.01$ versus glass, $n = 3$). The expression of Ret receptor is marginally increased on rGO substrates although not statistically significant due to the high variability of the rGO substrates. The expression of this gene on GO shows the same behaviour as the glass controls (figure 3*f*,*h*).

Faroni *et al.* [22] studied the gene expression changes when ASCs are differentiated towards Schwann-like dASCs. The gene expression of GDNF, BDNF, TrkC, Ret, nestin and vimentin markers was reported to be upregulated after the differentiation protocol compared to non-differentiated ASCs. The expression of NGF and TrkB was reported to be downregulated after the differentiation protocol compared to non-differentiated ASCs, although the level of NGF protein was found to be increased in the dASC phenotype.

The development of a protocol that permanently differentiates ASCs into dASCs is crucial to implement a stem cell-based therapy strategy for peripheral nerve regeneration. dASC cells were found able to express glial markers and to promote nerve regeneration, myelination and to increase the speed of the conduction in the nerve [8–11]. The main obstacle in the clinical translation of dASCs is the maintenance of the differentiated phenotype. Faroni *et al.* [22] proved that after the withdrawal of the growth factors, dASCs started to decrease the expression of glial markers and to reverse into ASC phenotype. There is consequently the need to develop better differentiation protocols and to test new materials that help maintaining the dASC phenotype even after the withdrawal of the growth factors for efficient delivery of stem cell therapies *in vivo*. Graphene and related nanomaterials have been widely reported as suitable material to support stem cell growth and differentiation [13–17]. In this study, the proliferation rate and the biocompatibility of these substrates were studied by two different assays and we can conclude that although there is a slower proliferation rate of dASCs on rGO and GO substrates, the amount of live cells is comparable between all the different substrates studied indicating that GO and rGO substrates do not cause cytotoxicity after 48 h. Importantly, the analysis of gene expression of important glial markers increased after 48 h of cellular growth on GO and rGO substrates. The expression of neurotrophins and their receptors is statistically increased on rGO substrates and to a lesser extent on GO substrates. Moreover, the expression of intermediate filament proteins such as nestin and vimentin is statistically increased on both GO and rGO substrates. Park *et al.* [36] reported increased neuronal differentiation of neural stem cells on graphene substrates together with decreased expression of glial cells. The contrast between our observations and previous results from Park *et al.* can be explained by the presence of laminin on the surface of the graphene coverslips. Laminin is a protein of the ECM which is reported to increase neuronal differentiation of embryonic and neural stem cells [37,38]. Previous results on ASC differentiation on GO substrates [13] showed enhanced osteogenesis, adipogenesis and epithelial genesis, but no experiment was conducted on rGO or graphene substrates. Our study points out the increased glial differentiation especially on rGO substrates. This is very interesting as specific properties of rGO can be exploitable in the clinical translation of dASCs. This is especially important for electrical conductivity as rGO compared to GO is not insulating and allows the possibility of electrically stimulating stem cells even in the presence of neuronal co-culture for peripheral nerve regeneration therapeutic strategy.

4. Conclusion

Our results confirm the biocompatibility of the graphene-based substrates and show increased expression of neurotrophins and filament proteins mainly on rGO and GO substrates. These results strongly position rGO and GO coatings to be used as functional surfaces to increase glial differentiation of ASCs at an earlier stage. As the initial results on 48 h are encouraging, further studies need to be conducted to establish if the gene expression of these markers will be increased at longer time points as the entire differentiation protocol required two weeks of treatment.

Ethics. All patients were fully consented and procedures approved by the National Research Ethics Committee, UK (NRES 13/SC/0499).

Data accessibility. This article has no additional data.

Authors' contributions. A.J.R., A.V. and A.F. conceived the experiments. A.F.V., A.F., M.I., C.S. and C.M. designed and carried out the experiments. All authors contributed to data analysis and co-wrote the paper.

Competing interests. We declare we have no competing interests.

Funding. A.V. and A.F.V. acknowledge funding from the Engineering and Physical Sciences Research Council (EPSRC) grant nos. EP/G03737X/1 and EP/K016946/1. C.S. acknowledges funding from Brazilian agency FAPESP (grant no. 2014/05048-4). A.F. and A.J.R. are supported by the Hargreaves and Ball Trust, the National Institute for Health Research (II-LA-0313-20003), the Academy of Medical Sciences and the Manchester Regenerative Medicine Network (MaRMN).

Acknowledgements. Thank you to Mr Jonathan Duncan and Miss Siobhan O'Ceallaigh (consultant plastic surgeons), and their patients at Wythenshawe Hospital, Manchester University NHS Foundation Trust for donation of adipose tissue, and to Acorda Therapeutics Inc, for kindly providing GGF-2.

References

1. Son YJ, Thompson WJ. 1995 Schwann cell processes guide regeneration of peripheral axons. *Neuron* **14**, 125–132. (doi:10.1016/0896-6273(95)90246-5)
2. Jessen KR, Mirsky R. 1991 Schwann cell precursors and their development. *Glia* **4**, 185–194. (doi:10.1002/glia.440040210)
3. Faroni A, Rothwell SW, Grolla AA, Terenghi G, Magnaghi V, Verkhratsky A. 2013 Differentiation of adipose-derived stem cells into Schwann cell phenotype induces expression of P2X receptors that control cell death. *Cell Death Dis.* **4**, e743. (doi:10.1038/cddis.2013.268)
4. Kingham PJ, Kalbermatten DF, Mahay D, Armstrong SJ, Wiberg M, Terenghi G. 2007 Adipose-derived stem cells differentiate into a Schwann cell phenotype and promote neurite outgrowth *in vitro*. *Exp. Neurol.* **207**, 267–274. (doi:10.1016/j.expneurol.2007.06.029)
5. Tomita K, Madura T, Mantovani C, Terenghi G. 2012 Differentiated adipose-derived stem cells promote myelination and enhance functional recovery in a rat model of chronic denervation. *J. Neurosci. Res.* **90**, 1392–1402. (doi:10.1002/jnr.23002)
6. Xu Y, Liu L, Li Y, Zhou C, Xiong F, Liu Z, Gu R, Hou X, Zhang C. 2008 Myelin-forming ability of Schwann cell-like cells induced from rat adipose-derived stem cells *in vitro*. *Brain Res.* **1239**, 49–55. (doi:10.1016/j.brainres.2008.08.088)
7. Mantovani C, Mahay D, Makam VS, Kingham PJ, Terenghi G, Shawcross SG, Wiberg M. 2010 Bone marrow- and adipose-derived stem cells show expression of myelin mRNAs and proteins. *Regen. Med.* **5**, 403–410. (doi:10.2217/rme.10.15)
8. Georgiou M, Golding JP, Loughlin AJ, Kingham PJ, Phillips JB. 2015 Engineered neural tissue with aligned, differentiated adipose-derived stem cells promotes peripheral nerve regeneration across a critical sized defect in rat sciatic nerve. *Biomaterials* **37**, 242–251. (doi:10.1016/j.biomaterials.2014.10.009)
9. di Summa PG, Kalbermatten DF, Pralong E, Raffoul W, Kingham PJ, Terenghi G. 2011 Long-term *in vivo* regeneration of peripheral nerves through bioengineered nerve grafts. *Neuroscience* **181**, 278–291. (doi:10.1016/j.neuroscience.2011.02.052)
10. di Summa PG, Kingham PJ, Raffoul W, Wiberg M, Terenghi G, Kalbermatten DF. 2010 Adipose-derived stem cells enhance peripheral nerve regeneration. *J. Plast. Reconstr. Aesthet. Surg.* **63**, 1544–1552. (doi:10.1016/j.bjps.2009.09.012)
11. di Summa PG, Kingham PJ, Campisi CC, Raffoul W, Kalbermatten DF. 2014 Collagen (NeuraGen®) nerve conduits and stem cells for peripheral nerve gap repair. *Neurosci. Lett.* **572**, 26–31. (doi:10.1016/j.neulet.2014.04.029)
12. Bussy C, Ali-Boucetta H, Kostarelos K. 2012 Safety considerations for graphene: lessons learnt from carbon nanotubes. *Acc. Chem. Res.* **46**, 692–701. (doi:10.1021/ar300199e)
13. Kim J *et al.* 2013 Bioactive effects of graphene oxide cell culture substratum on structure and function of human adipose-derived stem cells. *J. Biomed. Mater. Res. A* **101**, 3520–3530. (doi:10.1002/jbm.a.34659)
14. Lee WC, Lim CH, Shi H, Tang LA, Wang Y, Lim CT, Loh, KP. 2011 Origin of enhanced stem cell growth and differentiation on graphene and graphene oxide. *ACS Nano* **5**, 7334–7341. (doi:10.1021/nn202190c)
15. Yoo J, Kim J, Baek S, Park Y, Im H, Kim J. 2014 Cell reprogramming into the pluripotent state using graphene based substrates. *Biomaterials* **35**, 8321–8329. (doi:10.1016/j.biomaterials.2014.05.096)
16. Garcia-Alegria E *et al.* 2016 Graphene oxide promotes embryonic stem cell differentiation to haematopoietic lineage. *Sci. Rep.* **6**, 25917. (doi:10.1038/srep25917)
17. Nayak TR *et al.* 2011 Graphene for controlled and accelerated osteogenic differentiation of human mesenchymal stem cells. *ACS Nano* **5**, 4670–4678. (doi:10.1021/nn200500h)
18. Li N *et al.* 2011 The promotion of neurite sprouting and outgrowth of mouse hippocampal cells in culture by graphene substrates. *Biomaterials* **32**, 9374–9382. (doi:10.1016/j.biomaterials.2011.08.065)
19. Tang M, Song Q, Li N, Jiang Z, Huang R, Cheng G. 2013 Enhancement of electrical signaling in neural networks on graphene films. *Biomaterials* **34**, 6402–6411. (doi:10.1016/j.biomaterials.2013.05.024)
20. Tu Q, Pang L, Wang L, Zhang Y, Zhang R, Wang J. 2013 Biomimetic choline-like graphene oxide composites for neurite sprouting and outgrowth. *ACS Appl. Mater. Interfaces* **5**, 13 188–13 197. (doi:10.1021/am4042004)
21. Tu Q, Pang L, Chen Y, Zhang Y, Zhang R, Lu B, Wang J. 2014 Effects of surface charges of graphene oxide on neuronal outgrowth and branching. *Analyst* **139**, 105–115. (doi:10.1039/c3an01796f)
22. Faroni A, Smith RJP, Lu L, Reid AJ. 2016 Human Schwann-like cells derived from adipose-derived mesenchymal stem cells rapidly de-differentiate in the absence of stimulating medium. *Eur. J. Neurosci.* **43**, 417–430. (doi:10.1111/ejn.13055)
23. Marcano DC, Kosynkin DV, Berlin JM, Sinitskii A, Sun Z, Slesarev A, Alemany LB, Lu W, Tour JM. 2010 Improved synthesis of graphene oxide. *ACS Nano* **4**, 4806–4814. (doi:10.1021/nn1006368)
24. Hummers WS, Offeman RE. 1958 Preparation of graphitic oxide. *J. Am. Chem. Soc.* **80**, 1339. (doi:10.1021/ja01539a017)
25. Michio K, Hikaru T, Kazuto H, Shinsuke M, Chikako O, Asami F, Takaaki T, Yasumichi M. 2013 Analysis of reduced graphene oxides by X-ray photoelectron spectroscopy and electrochemical capacitance. *Chem. Lett.* **42**, 924–926. (doi:10.1246/cl.130152)
26. Ganguly A, Sharma S, Papakonstantinou P, Hamilton J. 2011 Probing the thermal deoxygenation of graphene oxide using high-resolution *in situ* X-ray-based spectroscopies. *J. Phys. Chem. C* **115**, 17 009–17 019. (doi:10.1021/jp203741y)
27. Hempstead BL. 2006 Dissecting the diverse actions of pro- and mature neurotrophins. *Curr. Alzheimer Res.* **3**, 19–24. (doi:10.2174/156720506775697061)
28. Reichardt LF. 2006 Neurotrophin-regulated signalling pathways. *Phil. Trans. R Soc. B* **361**, 1545–1564. (doi:10.1098/rstb.2006.1894)
29. Lentz SI, Knudson CM, Korsmeyer SJ, Snider WD. 1999 Neurotrophins support the development of diverse sensory axon morphologies. *J. Neurosci.* **19**, 1038–1048.
30. Sahin Kaya S, Mahmood A, Li Y, Yavuz E, Chopp M. 1999 Expression of nestin after traumatic brain injury in rat brain. *Brain Res.* **840**, 153–157. (doi:10.1016/S0006-8993(99)01757-6)
31. Frisén J, Johansson CB, Török C, Risling M, Lendahl U. 1995 Rapid, widespread, and longlasting induction of nestin contributes to the generation of glial scar tissue after CNS injury. *J. Cell Biol.* **131**, 453–464. (doi:10.1083/jcb.131.2.453)
32. Huaser S *et al.* 2011 Isolation of novel multipotent neural crest-derived stem cells from adult human inferior turbinate. *Stem Cells Dev.* **21**, 742–756. (doi:10.1089/scd.2011.0419)
33. Faroni A, Terenghi G, Magnaghi V. 2012 Expression of functional γ-aminobutyric acid type A receptors in Schwann-like adult stem cells. *J. Mol. Neurosci.* **47**, 619–630. (doi:10.1007/s12031-011-9698-9)
34. Amoh Y, Aki R, Hamada Y, Niiyama S, Eshima K, Kawahara K, Sato Y, Hoffman RM, Katsuoka K. 2012 Nestin-positive hair follicle pluripotent stem cells can promote regeneration of impinged peripheral nerve injury. *J. Dermatol.* **39**, 33–38. (doi:10.1111/j.1346-8138.2011.01413.x)
35. Perlson E, Hanz S, Ben-Yaakov K, Segal-Ruder Y, Seger R, Fainzilber M. 2005 Vimentin-dependent spatial translocation of an activated MAP kinase in injured nerve. *Neuron* **45**, 715–726. (doi:10.1016/j.neuron.2005.01.023)
36. Park SY, Park J, Sim SH, Sung MG, Kim KS, Hong BH, Hong S. 2011 Enhanced differentiation of human neural stem cells into neurons on graphene. *Adv. Healthc. Mater.* **23**, H263–H267. (doi:10.1002/adma.201101503)
37. Ma W, Tavakoli T, Derby E, Serebryakova Y, Rao MS, Mattson MP. 2008 Cell-extracellular matrix interactions regulate neural differentiation of human embryonic stem cells. *BMC Dev. Biol.* **8**, 90. (doi:10.1186/1471-213X-8-90)
38. Wilkinson AE, Kobelt LJ, Leipzig ND. 2013 Immobilized ECM molecules and the effects of concentration and surface type on the control of NSC differentiation. *J. Biomed. Mater. Res. A* **102**, 3419–3428. (doi:10.1002/jbm.a.35001)